

1 **An integrated user-friendly ArcMAP tool for bivariate statistical modeling in**  
2 **geoscience applications**

3  
4 **Mustafa Neamah Jebur, Biswajeet Pradhan\*, Helmi Zulhaidi Mohd Shafri, Zainuddin Md.**  
5 **Yusoff, Mahyat Shafapour Tehrani**

6 Department of Civil Engineering, Geospatial Information Science Research Center (GISRC),  
7 Faculty of Engineering,

8 University Putra Malaysia, 43400 UPM, Serdang, Selangor, Malaysia,

9 Tel. +603-89466383; Fax. +603-89468470

10 Email. [biswajeet24@gmail.com](mailto:biswajeet24@gmail.com) or [biswajeet@lycos.com](mailto:biswajeet@lycos.com) (corresponding author)

11  
12 **Abstract**

13  
14 Modeling and classification difficulties are fundamental issues in natural hazard assessment. A  
15 geographic information system (GIS) is a domain that requires users to use various tools to  
16 perform different types of spatial modeling. Bivariate statistical analysis (BSA) assists in hazard  
17 modeling. To perform this analysis, several calculations are required and the user has to transfer  
18 data from one format to another. Most researchers perform these calculations manually by using  
19 Microsoft Excel or other programs. This process is time consuming and carries a degree of  
20 uncertainty. The lack of proper tools to implement BSA in a GIS environment prompted this  
21 study. In this paper, a user-friendly tool, BSM (Bivariate statistical modeler), for BSA technique  
22 is proposed. Three popular BSA techniques such as frequency ratio, weights-of-evidence, and  
23 evidential belief function models are applied in the newly proposed ArcMAP tool. This tool is  
24 programmed in Python and created by a simple graphical user interface, which facilitates the  
25 improvement of model performance. The proposed tool implements BSA automatically, thus  
26 allowing numerous variables to be examined. To validate the capability and accuracy of this  
27 program, a pilot test area in Malaysia is selected and all three models are tested by using the  
28 proposed program. Area under curve is used to measure the success rate and prediction rate.  
29 Results demonstrate that the proposed program executes BSA with reasonable accuracy. The  
30 proposed BSA tool can be used in numerous applications, such as natural hazard, mineral  
31 potential, hydrological, and other engineering and environmental applications.

32 *Keywords:* ArcMAP tool, Bivariate statistical analysis, Geographic information systems

33  
34 **1 Introduction**

35  
36 Techniques to predict a response variable given a set of characteristics are required in several  
37 scientific regularities. Numerous applications have been implemented in various areas of  
38 geosciences. Bivariate analysis is one of the simplest methods of statistical analysis, and is

39 popular in numerous fields of study. Mathematicians, statisticians, biologists, and hydrologists  
40 use this method to perform their analysis. Different types of bivariate statistical analysis (BSA)  
41 have been established, for example, frequency ratio (FR), weights-of-evidence (WoE), and  
42 evidential belief function (EBF) (Yalcin, 2008). Although each of these methods requires  
43 specific mechanisms for calculation, all of these methods operate by using the same concept.  
44 Environmental scientists model various natural conditions by using the BSA statistical method.  
45 For instance, Ozdemir (2011) employed this technique for the same purpose. The results of the  
46 analysis were plotted in ArcGIS after computation in other programs. Mineral potential mapping  
47 is also aided by BSA techniques. Carranza (2004) used WoE modeling to map the mineral  
48 potential in the administrative province of Abra in northwestern Philippines. Their achievements  
49 indicate the plausibility of WoE in the mineral potential mapping of large areas with a small  
50 number of mineral prospects. Researchers have applied WoE in mapping mineral potential  
51 (Bonham-Carter et al., 1989) and remains popular in this area of research (Carranza et al., 2008).

52  
53 BSA is in demand in hazard studies because its procedure is simple and efficient. This technique  
54 is has been used in natural hazard applications by researchers to predict the spatial distribution of  
55 events. Extensive literature on different BSA techniques and their proficiency assessment are  
56 also available. BSA techniques can be used as a simple geospatial analysis tool to determine the  
57 probabilistic correlation among dependent variables (produced by using the inventory map of a  
58 hazard incidence) and independent variables (conditioning factors) containing multi-categorized  
59 maps (Oh et al., 2011). In BSA, the overlay of conditioning factors and computation of hazard  
60 densities, the significance of each factor, or the particular mixture of factors can be investigated  
61 individually. Bivariate statistical analysis functions by using a dependent variable and one  
62 conditioning factor. Hence, the significance of each factor is investigated separately (Porwal et  
63 al., 2006).

64  
65 In BSA, each conditioning factor is overlaid with the dependent variable. On the basis of the  
66 event density, weights are measured for each class of each factor. By using normalized weights  
67 (the correlation between the event density in each class of conditioning factor and the event  
68 density of the entire region), each conditioning factor is reclassified and the hazard map is  
69 produced. By using the acquired weights, decision rules can be produced on the basis of the  
70 knowledge of experts. Conditioning factors can also be combined to generate a map with  
71 uniform units, which is then overlaid with the inventory map to provide the density per class.  
72 The BSA approach has been used in landslide mapping (Constantin et al., 2011), earthquake  
73 studies (Xu et al., 2012b), flood susceptibility mapping (Tehrany et al., 2013), land subsidence  
74 (Kim et al., 2006; Lee and Park, 2013), and risk analysis (Hu et al., 2009). Numerous studies  
75 have been conducted to exploit the potential application of BSA in the hazard domain.

76  
77 This research examined the efficiency of statistical analysis, particularly bivariate analysis, in  
78 landslide studies in the Cuyahoga River watershed (Nandi and Shakoor, 2010). In another study,

79 FR and WoE were applied in the Sultan Mountains of southwestern Turkey to map areas that are  
80 susceptible to landslides (Ozdemir and Altural, 2013). According to Nandi and Shakoor (2010)  
81 and Ozdemir and Altural (2013), the BSA model is simple and its input, computation, and  
82 outcome procedures are effortlessly understood. The application of EBF in the area of landside  
83 studies has been investigated (Lee et al., 2013). Four functions, namely, degree of belief (Bel),  
84 degree of disbelief (Dis), degree of uncertainty (Unc) and degree of plausibility (Pls), are  
85 calculated separately to determine EBF.

86  
87 Each of these functions produces valuable information. However, each function requires  
88 individual computations with specific formulas. Tien Bui et al. (2012) used EBF and fuzzy logic  
89 methods in their research and found that the landslide susceptibility map derived from EBF has  
90 the highest prediction ability. They also established the efficiency of BSA in landslide mapping.  
91 BSA is also popular in hydrological research. Flood susceptibility maps assist in mitigation  
92 strategies. Lee et al. (2012) used the statistical method of FR to produce a map of flood-prone  
93 regions in Busan, Korea, in GIS. Tehrany et al. (2013) proposed an ensemble method of FR and  
94 LR to detect regions with high flood probability in Kelantan, Malaysia. The conditioning factors  
95 were reclassified on the basis of the weights acquired from the FR technique. These factors were  
96 entered in LR processing to obtain the MSA result. If the calculation time for these statistics can  
97 be reduced, the efficiency of the developed ensemble method will be enhanced. Hence,  
98 producing a tool that is capable of performing BSA calculations will help reduce the calculation  
99 time of ensemble methods.

100  
101 The BSA model has been widely used in land subsidence susceptibility mapping. In a study by  
102 Lee and Park (2013), the FR model was applied and compared with the machine learning of DT.  
103 The BSA is a method that is commonly used in natural hazard investigations. Although this  
104 method is not novel, the use of BSA has increased in recent years. RS and GIS have  
105 revolutionized the domain of natural hazards (Jebur et al., 2013a; Jebur et al., 2013b). Spatial  
106 database consists of different data types that are required to be transferred from one format to  
107 another because specific programs accept only specific data formats. Scientists have started to  
108 develop new programs in hazard studies because of the vital role of early warning systems in  
109 such applications (Osna et al., 2014; Pradhan et al., 2014). GIS is capable to store, analyze and  
110 show geographic information. It makes it possible to collect, organize, explore, model and view  
111 the spatial data for solving complex problems (Barreca et al., 2013). Different types of spatial  
112 data analysis ranges from the simple overlaying of various thematic layers to identify the region  
113 to the more complex use of mathematical equations or combined statistical models for the  
114 prediction of natural hazards. The importance of GIS in catastrophic evaluation was proven by  
115 many studies related to the GIS tools usages in exploration of various types of data (Steiniger  
116 and Hunter, 2013).

117 For example the existing hydrological GIS-based tools such as Mike SHE and ArcSWAT  
118 revealed considerable power in enhancing the accuracy of soil and water evaluations (Lei et al.,

119 2011). These tools are capable of facilitating the modeling and calibration procedure, and  
120 decreasing the stages in implementing the models and increasing the precision of the outcomes  
121 (Hörmann et al., 2009). The creation of tools that automatically implement susceptibility  
122 mapping was applied by Akgun et al. (2012). Akgun et al. (2012) proposed “MamLand,” a  
123 program in MATLAB, to create landslide susceptibility mapping by using fuzzy inference  
124 system. ArcGIS allows users to produce specific tools for spatial analysis (Stevens et al., 2007).  
125 For instance, Pradhan et al. (2014) developed a tool in ArcGIS to apply texture analysis for high-  
126 resolution radar data. Recently, a GIS-based system has been developed by Barreca et al. (2013)  
127 to evaluate and process the hazard associated to active faults influencing the eastern and southern  
128 flanks of Mt. Etna. The proposed tool was created in ArcGIS which contains various thematic  
129 datasets. It includes spatially-referenced arc-features and associated database. In another paper,  
130 Lei et al. (2011), integrated hydrological code EasyDHM and proposed open source  
131 MapWindow GIS tool called MWEasyDHM. Their aim was to create the tool by combining  
132 modules for preprocessing, modeling, viewing and analysis. MWEasyDHM tool is user friendly,  
133 free and proficient which produces selectable multi-functional hydrological analysis. Similarly, a  
134 number of GIS tools are programmed by Etherington (2011) in Python environment for  
135 landscape genetics researches. Tools are capable to transform files, view genetic relatedness, and  
136 calculate landscape associations through least-cost path procedure. The tools are free and  
137 available in ArcToolbox. In a separate paper, Roberts et al. (2010) implemented the research to  
138 facilitate the advanced analytic methods. A Marine Geospatial Ecology Tools (MGET) was  
139 created in GIS environment which is free, easy to use and efficient tools for the ecologists. The  
140 tools were made by integrating different strong programming methods of Python, R, MATLAB,  
141 and C++.

142  
143 The current research aims to reduce the processing time of BSA by introducing an easy-to-use  
144 ArcMap tool. On the basis of the aforementioned problem statement regarding the required  
145 processing time and difficulties for BSA, a program that is capable of calculating BSA  
146 automatically should be developed. Hence, a tool programmed in Python and based on the BSA  
147 technique is proposed. This tool automatically extracts the correlation among each class of  
148 conditioning factor and event occurrence, reclassifies the factors on the basis of the acquired  
149 weights in a GIS environment, and saves each correlation in separate folders. A simple graphical  
150 user interface (GUI) improves the model operation because Python knowledge is not required.  
151 The entire process can be performed in ArcGIS without any requirement for another program.  
152 The proposed tool was tested to generate a landslide susceptibility map of Bukit Antarabangsa,  
153 Ulu Klang, Malaysia.

## 154 155 **2 Methodology**

156 The procedural and theoretical perspectives of BSA applied in this research include several steps  
157 (Fig. 1). In the methodology flowchart, the BSA tool was developed and integrated into ArcGIS.

158 To apply BSA, the conditioning factors should be provided in raster format and classified with  
159 the proper scheme by the user. The BSA recognizes the effects of each class of conditioning  
160 factor on event occurrence. Hence, this step cannot be eliminated in the BSA process. As a  
161 second stage, a dependent variable (training layer) should be constructed by using the inventory  
162 map and other resources. This layer should contain a pixel value of one to represent the existence  
163 of an event. Once the conditioning factors are classified and the training layers are prepared, FR,  
164 WoE, and EBF can be applied automatically. The developed program reclassifies each  
165 conditioning factor by using the attained weights and saves them in a separate folder. The group  
166 of conditioning factors that have been assessed by BSA are ready to be entered in the raster  
167 calculator to derive the corresponding hazard map. The following sub-section represents the  
168 overall information on the scheme and functionality of the developed tool.

169 **Fig. 1.** About here

170

## 171 **2.1 Overall information on scheme and functionality**

172 The program is developed by using ArcGIS and Python for BSA. The tool can be used in  
173 ArcGIS 9 and 10 versions. Fig. 2 displays the interface of the tool in GIS toolbox.

174 **Fig. 2.** About here

175 The ArcToolbox provided in this research is used to enter the proposed tool in ArcMap. The user  
176 defines the source of the Python files of each model from the properties menu of the script (Fig.  
177 3).

178 **Fig. 3.** About here

179 The program is partitioned into three sections: FR, WoE, and EBF. The theoretical concept and  
180 graphic interface of each tool is discussed in the following sections.

### 181 **2.1.1 FR**

182 The theoretical expression of FR, as well as its usage in landslide susceptibility and flood  
183 mapping has been reported in the studies conducted by Yilmaz (2009) and Tehrany et al. (2013)  
184 respectively. The FR method has a simple and understandable structure compared with other  
185 probabilistic methods. FR is described as the proportion of the region where an event occurred  
186 over the entire area; FR is also defined as the proportion of likelihood of an event occurrence to a  
187 nonoccurrence for a particular attribute. FR can be calculated by using the following equation:

$$FR = \frac{\frac{N_{pix}(SX_i)}{\sum_{i=1}^m SX_i}}{N_{pix}(X_j)}}{\sum_{j=1}^n N_{pix}(X_j)} \quad (1)$$

188 where  $N_{pix}(SX_i)$  is the number of pixels, which contain an event in class  $i$  of the independent  
 189 variable;  $X$ ,  $N_{pix}(X_j)$  is the number of pixels and exist in independent variables  $X_j$ ;  $m$  is the  
 190 number of categoris of the independent variable  $X_i$ . Furthermore,  $n$  is the total number of  
 191 independent variables in the whole area (Yilmaz, 2009). Most of the researchers performed these  
 192 calculations manually by using Microsoft Excel or other programs. Once the weights were  
 193 obtained, these values were used to reclassify the independent variables by using the spatial  
 194 analyst tool in ArcGIS. The raster calculator in ArcGIS was used to obtain the final susceptibility  
 195 map. The proposed tool in ArcMap can apply the FR automatically and reclassify the  
 196 independent variables on the basis of the gained weights.  
 197

198 The graphic interface of the FR tool consists of one window containing four fields (Fig. 4). Each  
 199 field is user-defined in ArcGIS. The first field is the input raster, which is related to the desired  
 200 conditioning factor. The training layer or dependent variable, which is predefined and saved  
 201 prior to analysis, is selected for the second field. The cell size of the output and its location are  
 202 specified by the user in the third and fourth fields, respectively. The developed tool has a simple  
 203 structure, thus providing BSA for each conditioning factor within a few seconds. In manual  
 204 calculations, this procedure usually requires considerable amount of time to be implemented. The  
 205 proposed tool reclassifies the analyzed conditioning factor based on the attained weights and  
 206 saves it in the selected folder by the user.

207 **Fig. 4.** About here

### 208 2.1.2 WoE

209 The WoE method is a data-driven technique based on the Bayesian probability framework  
 210 (Beynon et al., 2000; Neuhäuser and Terhorst, 2007; Porwal et al., 2006). This characteristic  
 211 provides additional advantages to the proposed tool compared with other statistical methods. To  
 212 implement WoE, two important parameters of positive weight ( $W^+$ ) and negative weight ( $W^-$ )  
 213 are computed (Bonham-Carter et al., 1989). This technique calculates the weight for each  
 214 independent variable ( $B$ ) on the basis of the existence or non-existence of the event ( $A$ ) within  
 215 the study area (Xu et al., 2012a) by using the following equations:

$$W_i^+ = \ln \frac{P\{B|A\}}{P\{B|\bar{A}\}} \quad (2)$$

$$W_i^- = \ln \frac{P\{\bar{B}|A\}}{P\{\bar{B}|\bar{A}\}} \quad (3)$$

216 where  $P$  represents the probability,  $\ln$  is the natural *log*.  $B$ , and  $\bar{B}$  reveals the existence and  
 217 nonexistence of the independent variable.  $A$  and  $\bar{A}$  show the existence and nonexistence of the  
 218 event. A positive weight ( $W^+$ ) determines the presence of the specific independent variable at  
 219 the event, and the amount of positive weight represents the positive correlation between the

220 presence of the independent variable and event, respectively. A negative weight ( $W^-$ ) indicates  
221 the nonexistence of the independent variable and shows the amount of negative correlation.

222 The weight contrast is the difference between the two weights of  $W^+$  and  $W^-$ :

223

$$C(C = W^+ - W^-) \quad (6)$$

224

225 The size of the weight contrast demonstrates the spatial relationship between the independent  
226 variable and the event. The  $C$  value is positive in the case of a positive relationship and is  
227 negative in the case of a negative relationship.

228

229 The standard deviation of  $W$  is calculated as follows:

230

$$S(C) = \sqrt{S^2W^+ + S^2W^-} \quad (7)$$

231

232 where  $S(W^+)$  and  $S(W^-)$  are the variance of the positive and negative weights, respectively.

233 These variances can be calculated by using the following equations:

234

$$S^2W^+ = \frac{1}{N\{B \cap A\}} + \frac{1}{B \cap \bar{A}} \quad (8)$$

$$S^2W^- = \frac{1}{N\{\bar{B} \cap A\}} + \frac{1}{\{\bar{B} \cap \bar{A}\}} \quad (9)$$

235

236 By using the proportion of the contrast divided by its standard deviation, the studentized contrast  
237 is calculated. The studentized contrast is the final weight that assists the informal test if  $C$  is  
238 considerably different from zero or if the contrast is probable to be “real.” A complete  
239 explanation of the mathematical formulation of this method is accessible in Xu et al. (2012b).  
240 Fig. 5 illustrates the user interface of the WoE tool. Each field should be defined similar to FR.

241 **Fig. 5.** About here

242

### 243 2.1.3 EBF

244 Dempster (1967) is an innovator who presented the Dempster–Shafer theory of evidence, which  
245 is known as a generalized Bayesian theory of subjective probability. This theory has been used in  
246 several fields of study, including environmental and hazard studies (Awasthi and Chauhan,  
247 2011). This theory also has relative flexibility, which is considered its advantage, accepts  
248 uncertainty, and is capable of combining beliefs from different sources of evidence. EBF  
249 estimates the probability that a hypothesis is true and evaluates how close the evidence is to the  
250 truth of that hypothesis. A complex procedure is required to calculate EBF compared with FR.

251 To compute the EBF, four functions (Bel, Dis, Unc, and Pls) should be measured separately (Lee  
 252 et al., 2013). Individual computation by using specific formulas is required to provide this  
 253 information.

254 Assume that a set of independent variables of  $C = (C_i, i = 1, 2, 3, \dots, n)$ , which contains mutually  
 255 exclusive and exhaustive factors of  $C_i$ , is used in current research. The function  $m: P(C) \rightarrow [0,1]$   
 256 is the basic of the probability assignment.

257

$$\text{Bel}(C_{ij}) = \frac{W_{C_{ij}(\text{event})}}{\sum_{j=1}^n W_{C_{ij}(\text{event})}}, \quad (6)$$

258

259 where  $C$  is the frame of discernment and  $P(C)$  is the set of all subsets of  $C$ , counting the empty  
 260 set ( $\Phi$ ) and  $C$  itself. Mass function is another name for the mentioned function that satisfies  
 261  $m(\Phi) = 0$  and  $\sum_{A \subset C} m(A) = 1$ , where  $A$  is any subset of  $C$ . The degree in which the evidence  
 262 support  $A$  is calculated by  $m(A)$ , which is represented by a belief function ( $\text{Bel}(A)$ ). Suppose that  
 263  $N(L)$  and  $N(C)$  are the total number of pixels affected by the event and the total number of pixels  
 264 in the study area, respectively;  $C_{ij}$  is the  $j$ -th class of the independent variable of  $C_i$  ( $i =$   
 265  $1, 2, 3, \dots, n$ );  $N(C_{ij})$  is the total number of pixels in class  $C_{ij}$ ; and  $N = (L \cap C_{ij})$  is the number of  
 266 pixels affected by the event in  $C_{ij}$ . Therefore, the data-driven measurements of EBF can be  
 267 calculated using equation 6 and the following equation (Tien Bui et al., 2012):

$$W_{C_{ij}(\text{event})} = \frac{N(L \cap C_{ij}) / N(L)}{[N(C_{ij}) - N(L \cap C_{ij})] / [N(C) - N(L)]} \quad (7)$$

$$\text{Dis}(C_{ij}) = \frac{W_{C_{ij}}(\text{Non - even})}{\sum_{j=1}^n W_{C_{ij}}(\text{Non - even})} \quad (8)$$

268 where the  $C_{ij}$  is shown by  $W_{C_{ij}(\text{event})}$  and supports the belief that the presence of the event is  
 269 more than its nonexistence. The detailed mathematical calculation of each function has been  
 270 discussed in several studies, such as Lee et al. (2013). Fig. 6 represents the interface of the EBF  
 271 tool, and contains three more fields compared with the two other methods because each EBF  
 272 function should be applied and saved in a separate folder. Hence, after the selection of the  
 273 conditioning factor, training layer, and output cell size, the location to save each function should  
 274 be defined.

275

276 **Fig. 6.** About here

277



## 278 2.2 Code description

279 The code was designed in python 27 (The default software included with windows 7). In the  
280 beginning, the arcpy library is called to check the code for spatial extension in order to continue  
281 the process. After that, when the user defines the raster, the code calls the raster data as text  
282 using the command “GetParameterAsText” which is part of arcpy library. Using same as the  
283 previous command, the code will define the output layer for the chosen model. The default path  
284 for all the sub process is defined to be in “C” drive because it is the default drive in all the  
285 systems. Therefore, the code creates folder calls “FR\_modeler”, "WOE\_modeler", or  
286 "EBF\_modeler" depending on the selected process.

287 The next stage is to analyze the input layer (e.g. Slope) and “Lookup” command will be applied  
288 to prepare the layer for zonal geometry process. The zonal geometry is defined as table to be able  
289 to work on the statistic of the output. A field is added to the attribute of the created table in the  
290 previous step namely “zonal” to be used for calculating the percentage of each class of the input  
291 layer. A statistics analysis was applied to calculate the sum of all the pixels of the selected layer.  
292 Then, a joining process is defined to link the created table with the input layer. Subsequently,  
293 tabulate area process was ran to calculate the percentage of the occurrence of the independent  
294 factor (i.e. Landslide) in each input layer classes. The last step for calculating FR is applied using  
295 eq.1. Then, the resulted values is defined as integer and used to reclassify the input layer. The  
296 code includes a delete command to delete all the sub process layers and table.

297 The process of WoE and EBF contains the same process of FR as initial step. However, more  
298 statistical analysis and more field are added to calculate the parameters of WoE and EBF which  
299 is listed in eq. (2-8). In each selected model, a different folder will be created. The user may  
300 overwrite and redo the process as much as required because the command “overwriteOutput”  
301 was defined for each code. The flow chart regarding the three algorithms is shown in fig 7, 8,  
302 and 9.

303 **Fig. 7.** About here

304

305 **Fig. 8.** About here

306

307 **Fig. 9.** About here

308

## 309 2.3 Test area and data

310 Although the developed program can be used in any application that employs BSA, the  
311 proficiency of the tool was tested in the hazard domain. To examine the capability and efficiency  
312 of the developed program, landslide susceptibility analyses were performed by using the  
313 developed ArcMAP tool with three BSA models, namely, FR, WoE, and EBF. The program was

314 tested for the landslide susceptibility mapping of Bukit Antarabangsa, Ulu Klang, Malaysia (Fig.  
315 10).

316

317 **Fig. 10.** About here

318

319 A spatial database was constructed and analyzed on the basis of the altitude, aspect, curvature,  
320 slope, stream power index, topographic wetness index, distance from the river, distance from the  
321 road, and geological layers. Comprehensive overview of the usage of BSA for landslide  
322 susceptibility mapping has been reported in numerous studies (Yalcin et al., 2011). Study  
323 conducted by Mohammady et al. (2012) provided additional knowledge on the capabilities of  
324 these three BSA methods. These previous research compared the three methods of FR, WoE, and  
325 EBF and determined the pros and cons of each statistical approach. A total of 47 landslide  
326 locations were recorded and a landslide inventory map was prepared. The allocation of the  
327 landslide inventory for training and testing was 70% and 30%, respectively (Fig. 10). The  
328 training data set (31 landslide locations) was chosen randomly and a dependent layer (landslide  
329 layer) was created.

330

### 331 **3 Experimental results and discussion**

332 To examine the efficiency of the developed BSM tool, landslide susceptibilities were derived by  
333 using all three methods. The correlation among the conditioning factors and landslide occurrence  
334 was extracted. The landslide probability index was measured and classified by using the proper  
335 scheme. To produce a susceptibility map, the probability index should be partitioned into various  
336 classes. The quantile method was applied in the current research because of its reputation in  
337 classification. In the quantile classification method, each class has the same number of features.  
338 This method has been employed by several researchers, such as Umar et al. (2014) and  
339 Papadopoulou-Vrynioti et al. (2014). The method provided appropriate results on the comparison  
340 between the created landslide susceptibility map and the spatial distribution of landslide events.  
341 The acquired landslide conditioning factors is shown in Fig. 11.

342

343 **Fig. 11.** About here

344

345 The derived landslide susceptibility map from WoE shows a different appearance compared with  
346 the two other maps. Validation should be performed to determine which map is reliable. The area  
347 under curve (AUC) was applied to examine the precision of the derived susceptibility maps  
348 (Pérez-Vega et al., 2012). The success rate values were 68%, 63%, and 76% for FR, WoE, and  
349 EBF, respectively. Moreover, 71%, 75%, and 80% were the prediction rates for FR, WoE, and  
350 EBF, respectively. The EBF represented the highest accuracy compared with other methods in  
351 terms of success and prediction rates. The prediction rate value for WoE was high but not as high  
352 as EBF. This result is caused by the greater proficiency and capability of EBF compared with  
353 WoE. Recognizing the best method for modeling is possible because any comparative study is

354 restricted and the best method for a specific data set is significantly related to the characteristics  
355 of that dataset. Fig. 12 illustrates the computed accuracies.

356

357 **Fig. 12.** About here

358

359 The design and interface of the developed tool show that the BSA is simple to execute by using  
360 the proposed program compared with manual calculation. The derived susceptibility maps and  
361 their AUC values suggest that the tool is precise and reliable. Previous research has established  
362 that because of the nature of BSA, the obtained results are imprecise compared with machine  
363 learning and rule-based methods. Therefore, the measured accuracies are acceptable for these  
364 simple statistical methods.

365

#### 366 **4 Conclusion**

367 To perform hazard studies, several requirements, such as constructing the precise spatial  
368 database, obtaining high-resolution imagery, and providing a reliable inventory map, should be  
369 fulfilled. Users can be confronted with the insufficiency of appropriate and free tools to perform  
370 various analyses. This condition makes such studies complex and in some cases, time  
371 consuming. The BSA is one of the fundamental methods in hazard mapping. Hence, developing a  
372 tool that manages a large number of factors with an automatic statistical and classification  
373 performance is essential. Users commonly have to apply the BSA calculation manually and  
374 within separate software. The results have to be entered in a GIS environment and used to  
375 reclassify each conditioning factor one after another. The proposed BSM tool can be used to  
376 automate the BSA procedure and to facilitate the generation of the probability index. BSM is  
377 developed as a tool in ArcGIS, which is capable of performing the three BSA models of FR,  
378 WoE, and EBF. This tool can also manage large amounts of conditioning factors with reduced  
379 calculation time, thus allowing the replication of various trials. As an example, a significant  
380 characteristic of BSM is the reclassification of the conditioning factors on the basis of the  
381 acquired weight from BSA. The GUI also allows the application of RF, WoE, and EBF without  
382 entering any code from Python, thus helping the user in model operation. The application to  
383 landslide susceptibility mapping in Bukit Antarabangsa in Ulu Klang, Malaysia provides  
384 significant outcomes. All three methods are applied and landslide susceptibility maps are created.  
385 FR, WoE, and EBF acquired success rates of 68%, 63%, and 76%, respectively. AUC values for  
386 prediction rates are 71%, 75%, and 80% for FR, WoE, and EBF, respectively. In conclusion, the  
387 proposed tool can transform the BSA procedure into a simple and fast technique. This tool can  
388 assist scientists in performing statistical analyses for any environment and mathematical  
389 application.

390

391

392

393

394 **References**

- 395 Akgun, A., Sezer, E. A., Nefeslioglu, H. A., Gokceoglu, C., Pradhan, B.: An easy-to-use MATLAB  
396 program (MamLand) for the assessment of landslide susceptibility using a Mamdani fuzzy  
397 algorithm, *Comput. Geosci.*, 38, 23-34, 2012.
- 398 Awasthi, A., Chauhan, S. S.: Using AHP and Dempster–Shafer theory for evaluating sustainable transport  
399 solutions, *Environ. Modell. Softw.*, 26, 787-796, 2011.
- 400 Barreca, G., Bonforte, A., Neri, M.: A pilot GIS database of active faults of Mt. Etna (Sicily): A tool for  
401 integrated hazard evaluation, *J. Volcanol. Geoth. Res.*, 251, 170-186, 2013.
- 402 Beynon, M., Curry, B., Morgan, P.: The Dempster–Shafer theory of evidence: an alternative approach to  
403 multicriteria decision modelling, *Omega.*, 28, 37-50, 2000.
- 404 Bonham-Carter, G. F., Agterberg, F. P., Wright, D. F.: Weights of evidence modelling: a new approach to  
405 mapping mineral potential, *Comput. Geol.*, 89, 171–183, 1989.
- 406 Carranza, E. J. M.: Weights of evidence modeling of mineral potential: a case study using small number  
407 of prospects, Abra, Philippines, *Nat. Resour. Res.*, 13, 173-187, 2004.
- 408 Carranza, E. J. M., Van Ruitenbeek, F., Hecker, C., van der Meijde, M., van der Meer, F. D.: Knowledge-  
409 guided data-driven evidential belief modeling of mineral prospectivity in Cabo de Gata, SE  
410 Spain, *Int. J. Appl. Earth. Obs.*, 10, 374-387, 2008.
- 411 Constantin, M., Bednarik, M., Jurchescu, M. C., Vlaicu, M.: Landslide susceptibility assessment using the  
412 bivariate statistical analysis and the index of entropy in the Sibiciu Basin (Romania), *Environ.*  
413 *Earth. Sci.*, 63, 397-406, 2011.
- 414 Dempster, A. P.: Upper and lower probabilities induced by a multivalued mapping, *Ann. Math. Stat.*, 325-  
415 339, 1967.
- 416 Etherington, T. R.: Python based GIS tools for landscape genetics: visualising genetic relatedness and  
417 measuring landscape connectivity, *Methods. Ecol. Evol.*, 2, 52-55, 2011.
- 418 Hörmann, G., Köplin, N., Cai, Q., Fohrer, N.: Using a simple model as a tool to parameterise the SWAT  
419 model of the Xiangxi river in China, *Quatern. Int.*, 208, 116-120, 2009.
- 420 Hu, B., Zhou, J., Wang, J., Chen, Z., Wang, D., Xu, S.: Risk assessment of land subsidence at Tianjin  
421 coastal area in China, *Environ. Earth. Sci.*, 59, 269-276, 2009.
- 422 **Jebur, M. N., Pradhan, B., Tehrany, M. S.: Detection of vertical slope movement in highly vegetated**  
423 **tropical area of Gunung pass landslide, Malaysia, using L-band InSAR technique, *Geosci. J.*, 18,**  
424 **61-68, 2013a.**
- 425 **Jebur, M. N., Pradhan, B., Tehrany, M. S.: Using ALOS PALSAR derived high-resolution DInSAR to**  
426 **detect slow-moving landslides in tropical forest: Cameron Highlands, Malaysia, *Geomat. Nat.***  
427 ***Hazards. Risk.*, 1-19, doi:10.1080/19475705.2013.860407, 2013b.**
- 428 Kim, K. D., Lee, S., Oh, H. J., Choi, J. K., Won, J. S.: Assessment of ground subsidence hazard near an  
429 abandoned underground coal mine using GIS, *Environ. Geol.*, 50, 1183-1191, 2006.
- 430 Lee, M. J., Kang, J. e., Jeon, S.: Application of frequency ratio model and validation for predictive  
431 flooded area susceptibility mapping using GIS, in: *IEEE International Geoscience and Remote*  
432 *Sensing Symposium (IGARSS)*, Munich, 895-898, 2012.
- 433 Lee, S., Hwang, J., Park, I.: Application of data-driven evidential belief functions to landslide  
434 susceptibility mapping in Jinbu, Korea, *Catena.*, 100, 15-30, 2013.
- 435 Lee, S., Park, I.: Application of decision tree model for the ground subsidence hazard mapping near  
436 abandoned underground coal mines, *J. Environ. Manage.*, 127, 166-176, 2013.
- 437 Lei, X., Wang, Y., Liao, W., Jiang, Y., Tian, Y., Wang, H.: Development of efficient and cost-effective  
438 distributed hydrological modeling tool MWEasyDHM based on open-source MapWindow GIS,  
439 *Comput. Geosci.*, 37, 1476-1489, 2011.
- 440 **Mohammady, M., Pourghasemi, H. R., Pradhan, B.: Landslide susceptibility mapping at Golestan**  
441 **Province, Iran: a comparison between frequency ratio, Dempster–Shafer, and weights-of-**  
442 **evidence models, *J. Asian. Earth. Sci.*, 61, 221-236, 2012.**

443 Nandi, A., Shakoor, A.: A GIS-based landslide susceptibility evaluation using bivariate and multivariate  
444 statistical analyses, *Eng. Geol.*, 110, 11-20, 2010.

445 Neuhäuser, B., Terhorst, B.: Landslide susceptibility assessment using “weights-of-evidence” applied to a  
446 study area at the Jurassic escarpment (SW-Germany), *Geomorphology.*, 86, 12-24, 2007.

447 Oh, H. J., Kim, Y. S., Choi, J. K., Park, E., Lee, S.: GIS mapping of regional probabilistic groundwater  
448 potential in the area of Pohang City, Korea, *J. Hydrol.*, 399, 158-172, 2011.

449 Osna, T., Sezer, E. A., Akgun, A.: GeoFIS: An Integrated Tool for the Assessment of Landslide  
450 Susceptibility, *Comput. Geosci.*, 66, 20-30, 2014.

451 Ozdemir, A.: Using a binary logistic regression method and GIS for evaluating and mapping the  
452 groundwater spring potential in the Sultan Mountains (Aksehir, Turkey), *J. Hydrol.*, 405, 123-  
453 136, 2011.

454 Ozdemir, A., Altural, T.: A comparative study of frequency ratio, weights of evidence and logistic  
455 regression methods for landslide susceptibility mapping: Sultan Mountains, SW Turkey, *J. Asian  
456 Earth. Sci.*, 64, 180-197, 2013.

457 Pérez-Vega, A., Mas, J. F., Ligmann-Zielinska, A.: Comparing two approaches to land use/cover change  
458 modeling and their implications for the assessment of biodiversity loss in a deciduous tropical  
459 forest, *Environ. Modell. Softw.*, 29, 11-23, 2012.

460 Porwal, A., Carranza, E., Hale, M.: Bayesian network classifiers for mineral potential mapping, *Comput.  
461 Geosci.*, 32, 1-16, 2006.

462 Pradhan, B., Hagemann, U., Shafapour Tehrany, M., Prechtel, N.: An easy to use ArcMap based texture  
463 analysis program for extraction of flooded areas from TerraSAR-X satellite image, *Comput.  
464 Geosci.*, 63, 34-43, 2014.

465 Roberts, J. J., Best, B. D., Dunn, D. C., Treml, E. A., Halpin, P. N.: Marine Geospatial Ecology Tools: An  
466 integrated framework for ecological geoprocessing with ArcGIS, Python, R, MATLAB, and C++,  
467 *Environ. Modell. Softw.*, 25, 1197-1207, 2010.

468 Steiniger, S., Hunter, A. J.: The 2012 free and open source GIS software map—A guide to facilitate  
469 research, development, and adoption, *Comput. Environ. Urban.*, 39, 136-150, 2013.

470 Stevens, D., Dragicevic, S., Rothley, K.: < i> iCity</i>: A GIS—CA modelling tool for urban planning and  
471 decision making, *Environ. Modell. Softw.*, 22, 761-773, 2007.

472 Tehrany, M. S., Pradhan, B., Jebur, M. N.: Spatial prediction of flood susceptible areas using rule based  
473 decision tree (DT) and a novel ensemble bivariate and multivariate statistical models in GIS, *J.  
474 Hydrol.*, 504, 69-79, 2013.

475 Tien Bui, D., Pradhan, B., Lofman, O., Revhaug, I., Dick, O. B.: Spatial prediction of landslide hazards in  
476 Hoa Binh province (Vietnam): a comparative assessment of the efficacy of evidential belief  
477 functions and fuzzy logic models, *Catena.*, 96, 28-40, 2012.

478 Xu, C., Xu, X., Dai, F., Xiao, J., Tan, X., Yuan, R.: Landslide hazard mapping using GIS and weight of  
479 evidence model in Qingshui river watershed of 2008 Wenchuan earthquake struck region, *J.  
480 Earth. Sci.*, 23, 97-120, 2012a.

481 Xu, C., Xu, X., Lee, Y. H., Tan, X., Yu, G., Dai, F.: The 2010 Yushu earthquake triggered landslide  
482 hazard mapping using GIS and weight of evidence modeling, *Environ. Earth. Sci.*, 66, 1603-1616,  
483 2012b.

484 Yalcin, A.: GIS-based landslide susceptibility mapping using analytical hierarchy process and bivariate  
485 statistics in Ardesen (Turkey): comparisons of results and confirmations, *Catena*, 72, 1-12, 2008.

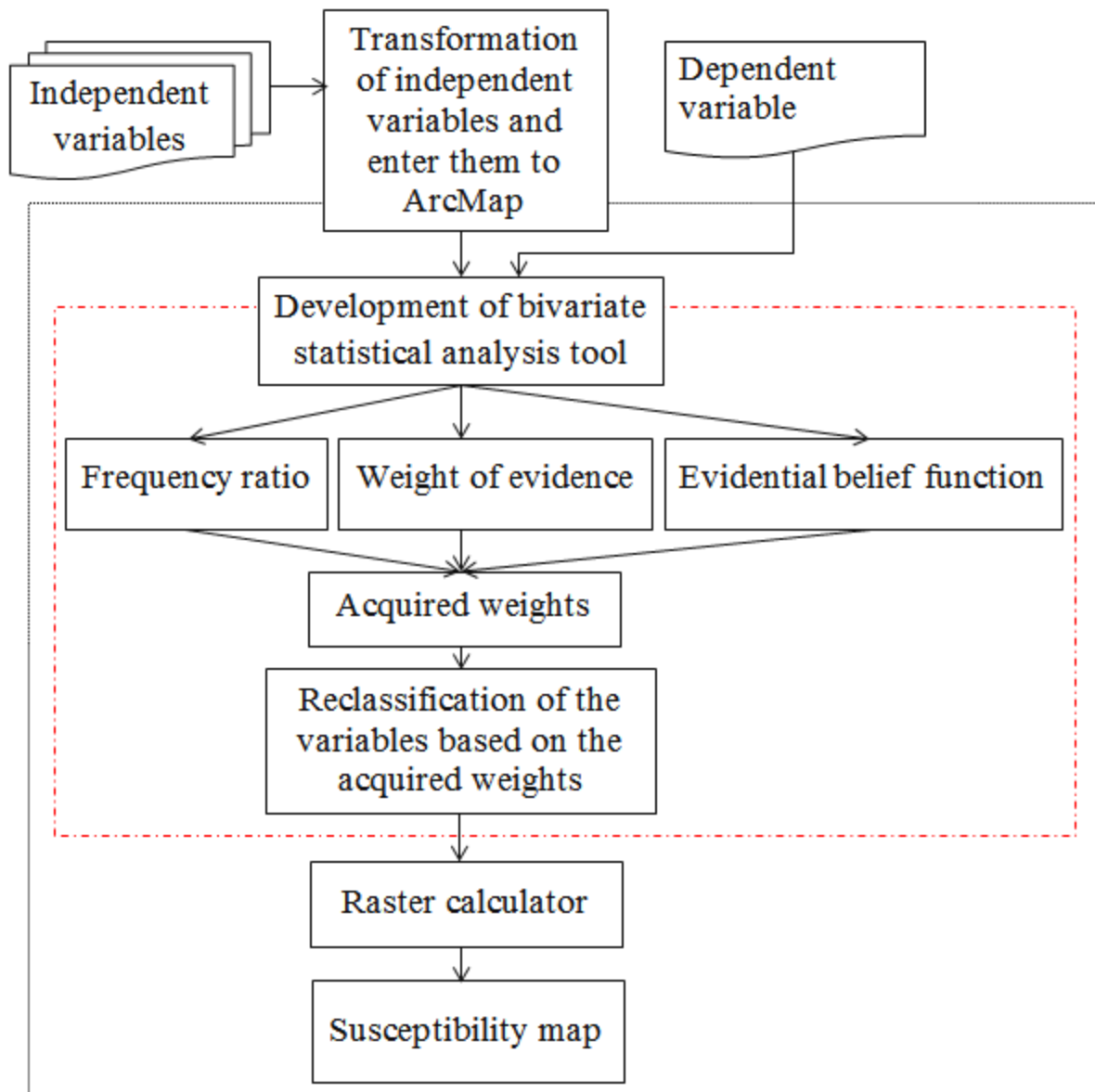
486 Yalcin, A., Reis, S., Aydinoglu, A., Yomralioglu, T.: A GIS-based comparative study of frequency ratio,  
487 analytical hierarchy process, bivariate statistics and logistics regression methods for landslide  
488 susceptibility mapping in Trabzon, NE Turkey, *Catena.*, 85, 274-287, 2011.

489 Yilmaz, I.: Landslide susceptibility mapping using frequency ratio, logistic regression, artificial neural  
490 networks and their comparison: a case study from Kat landslides (Tokat—Turkey), *Comput.  
491 Geosci.*, 35, 1125-1138, 2009.

492

493

494

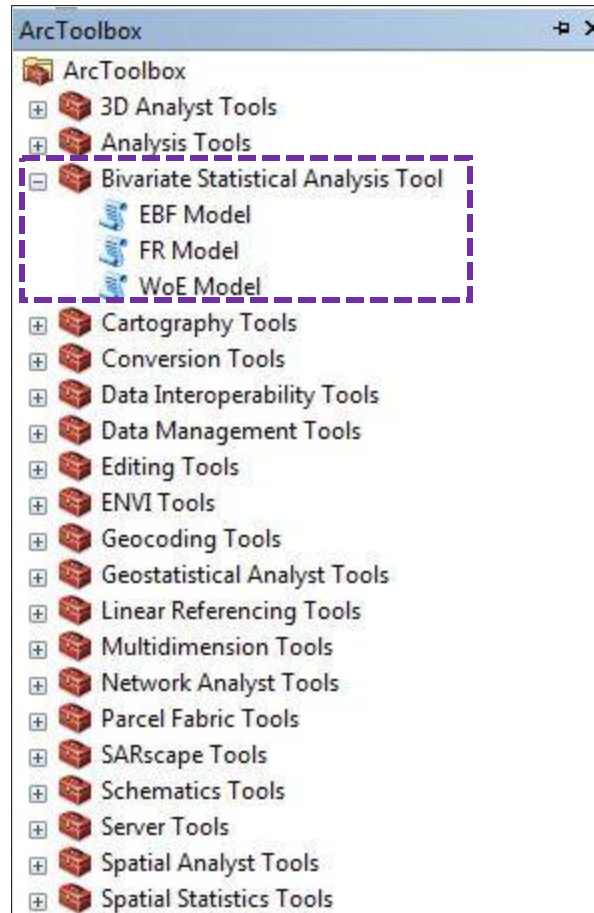


495

496

497

**Fig. 1.** General design of the methodology and BSA tool.



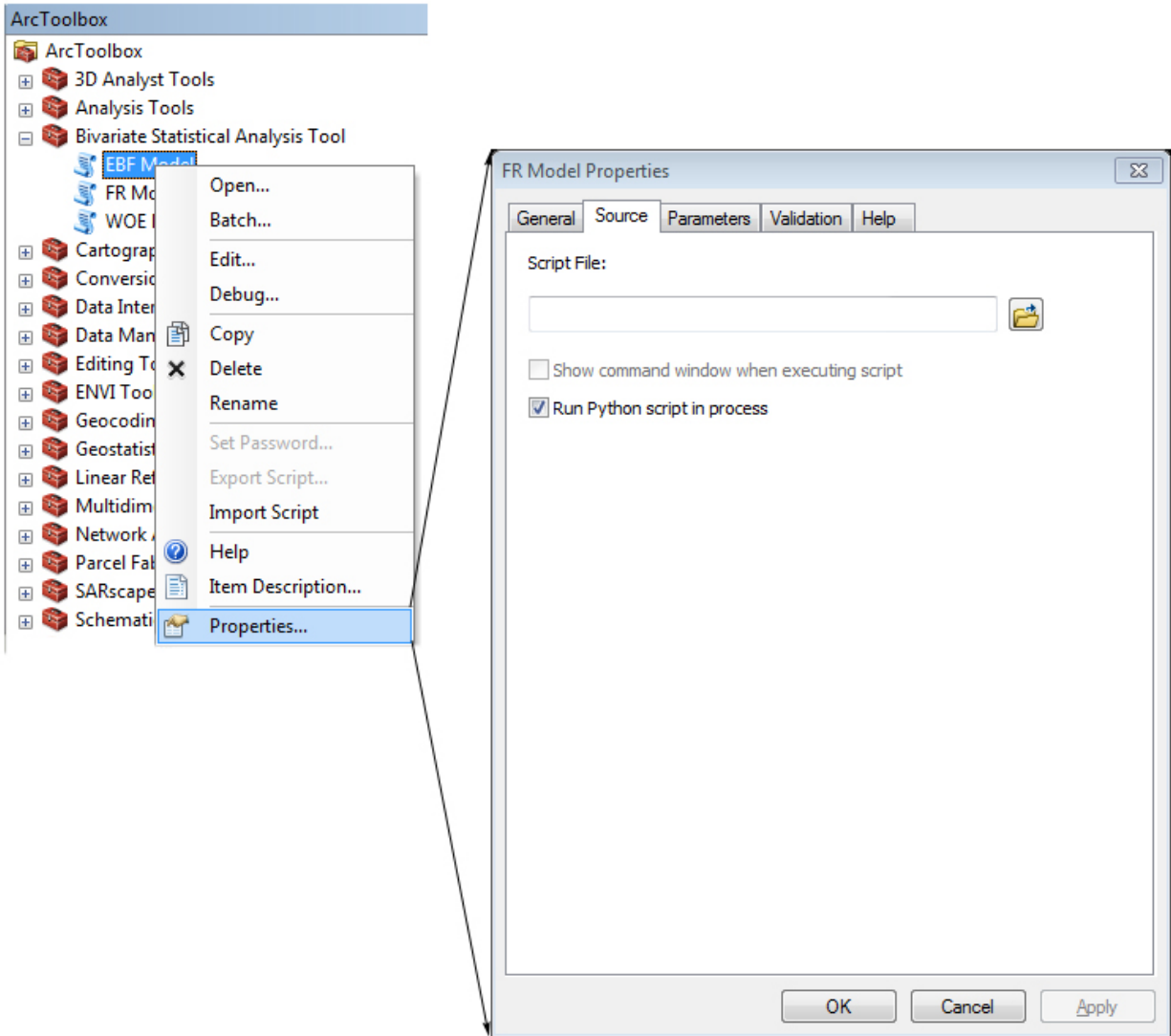
498

499

500

**Fig. 2.** BSA tool interface.



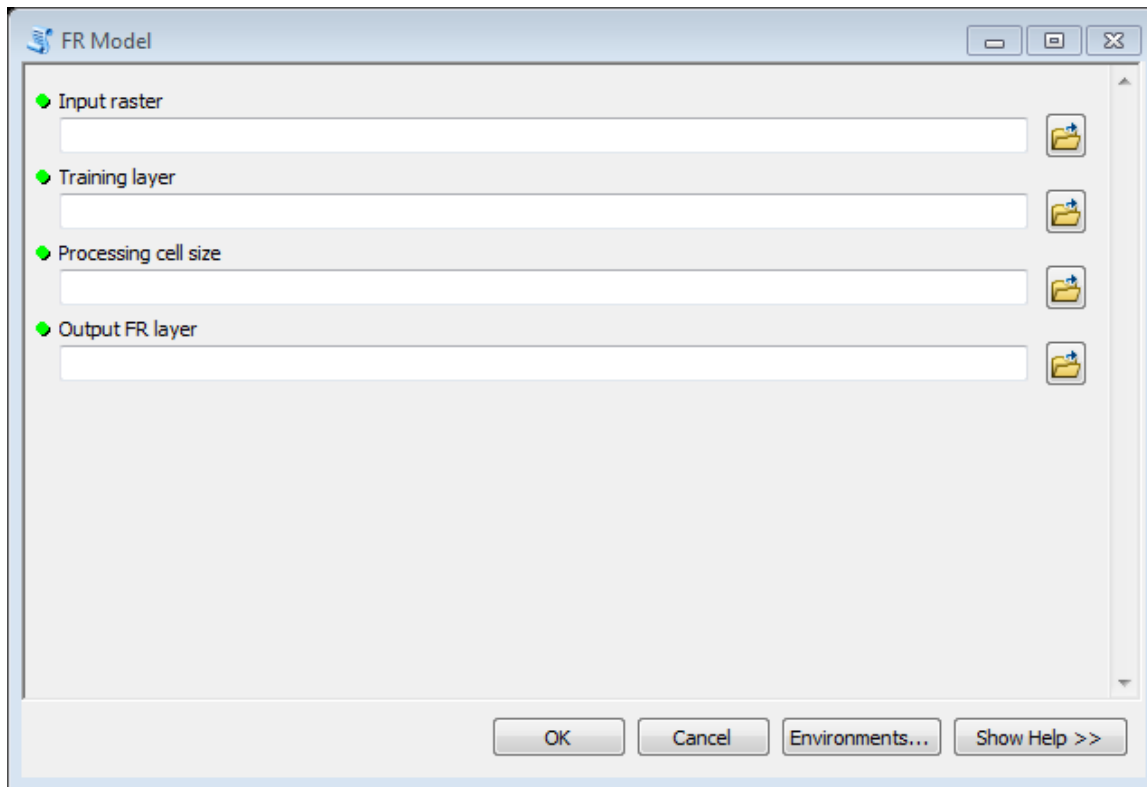


501

502

503

**Fig. 3.** Procedure to add the BSM tool in ArcGIS.

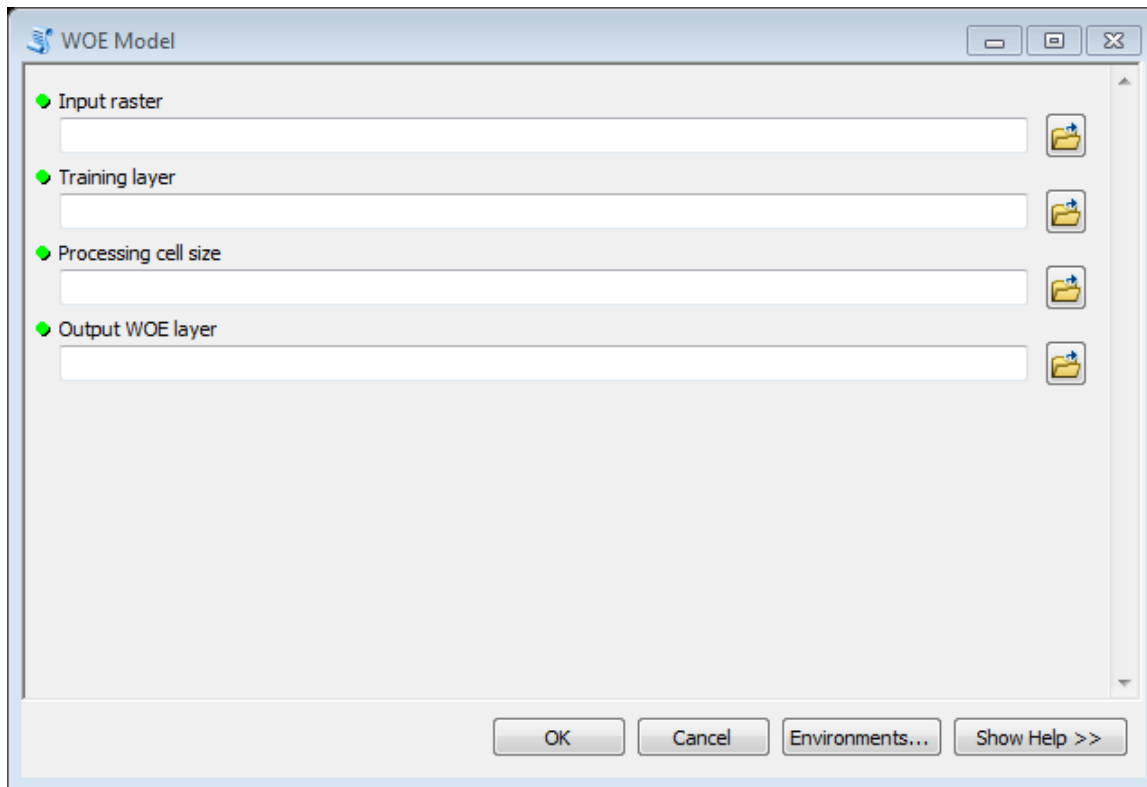


504

505

506

**Fig. 4.** Graphic user interface of the FR tool.

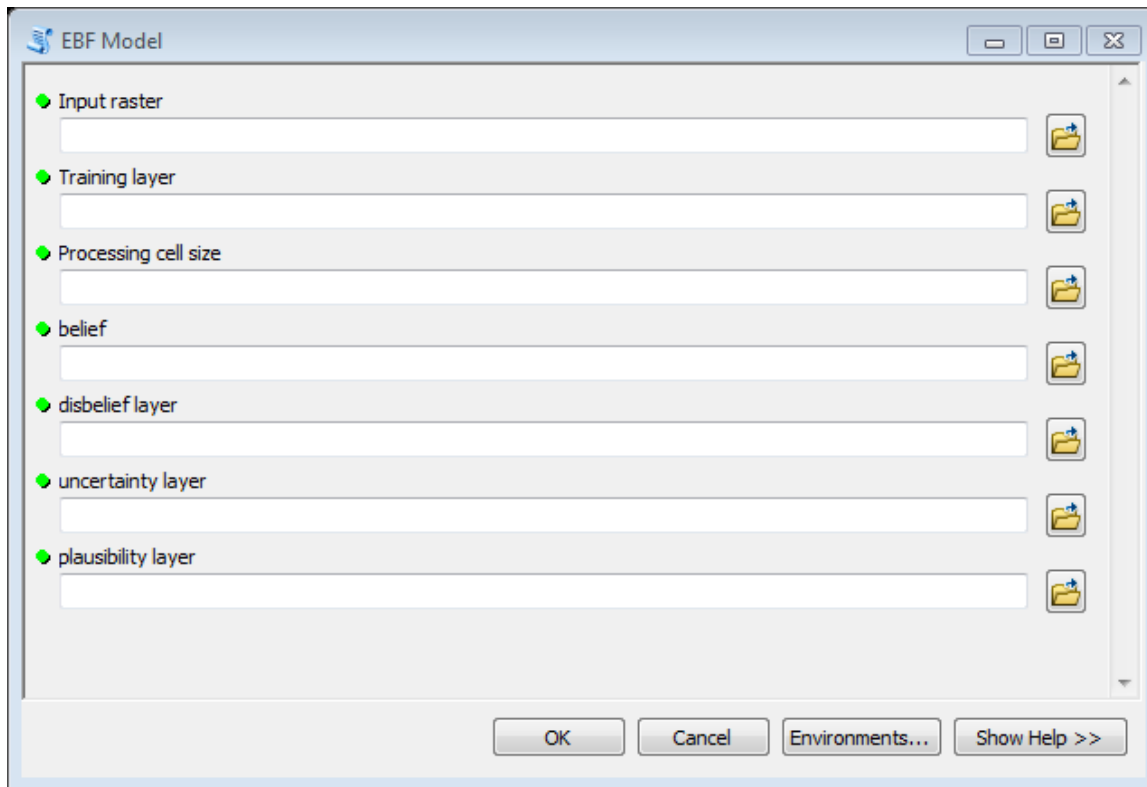


507

508

509

**Fig. 5.** Graphic interface of the WoE tool.



510

511

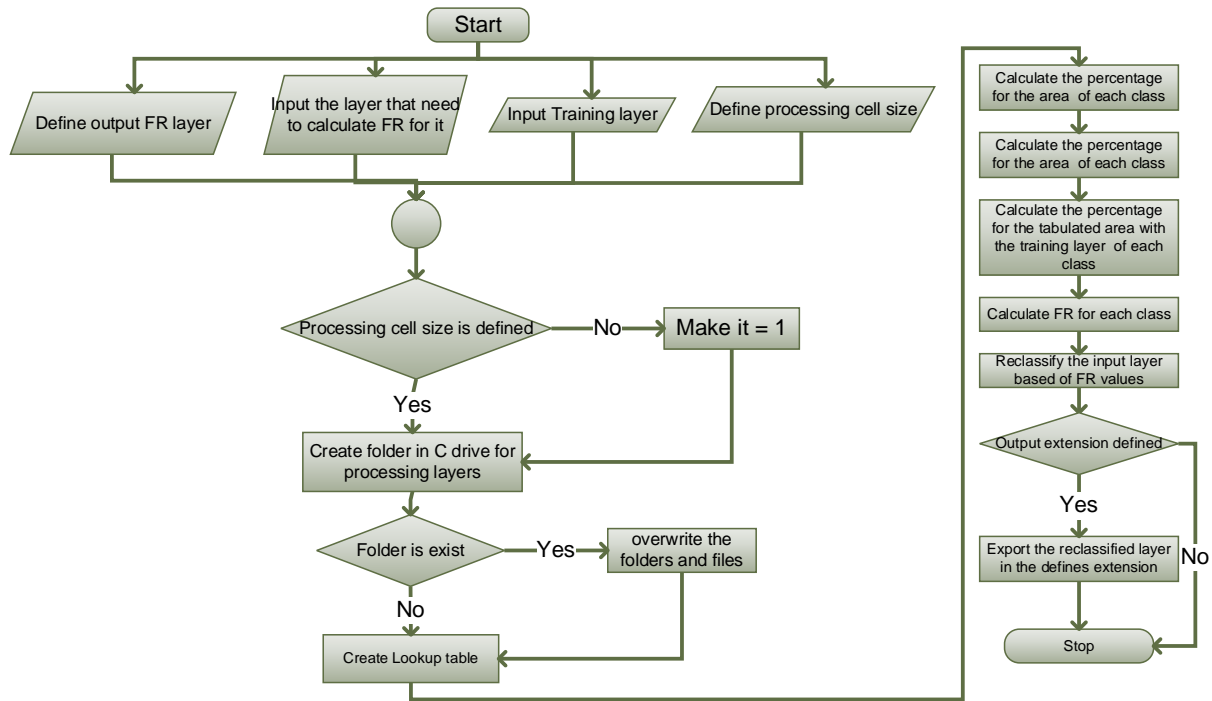
**Fig. 6.** Graphic interface of the EBF tool.

512

513

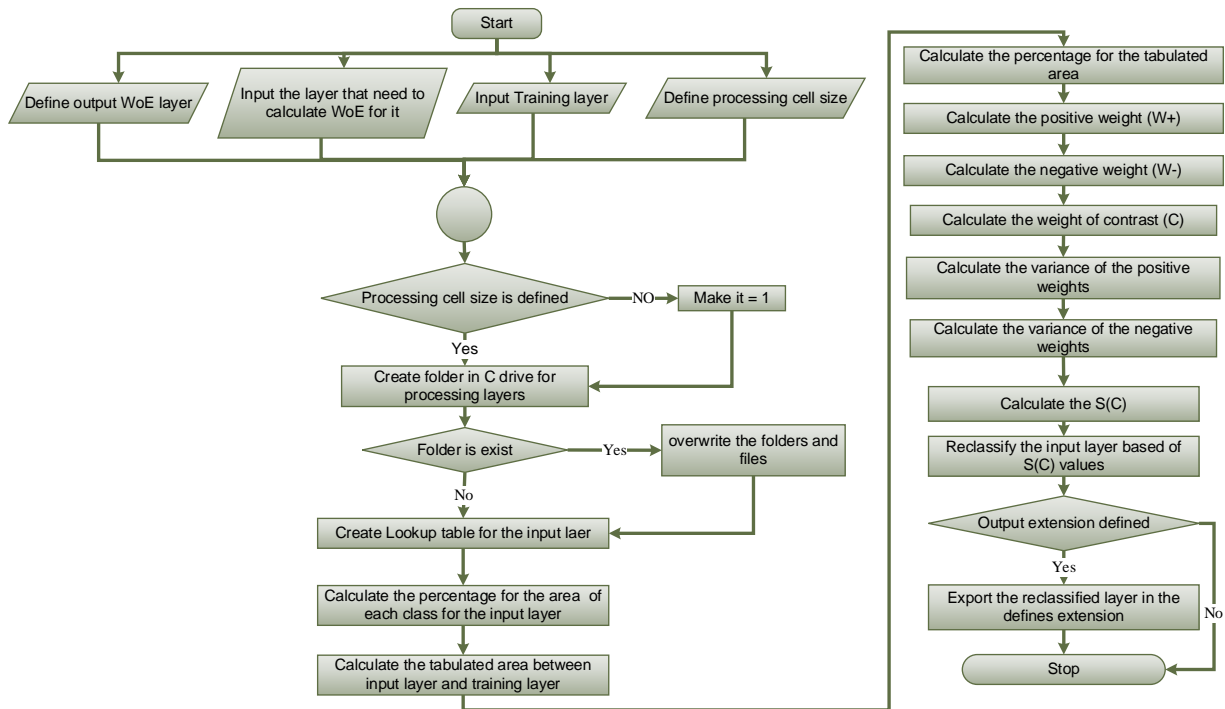
514

515



516  
517

**Fig. 7.** Code flowchart of the FR model.



518  
519

**Fig. 8.** Code flowchart of the WoE model.

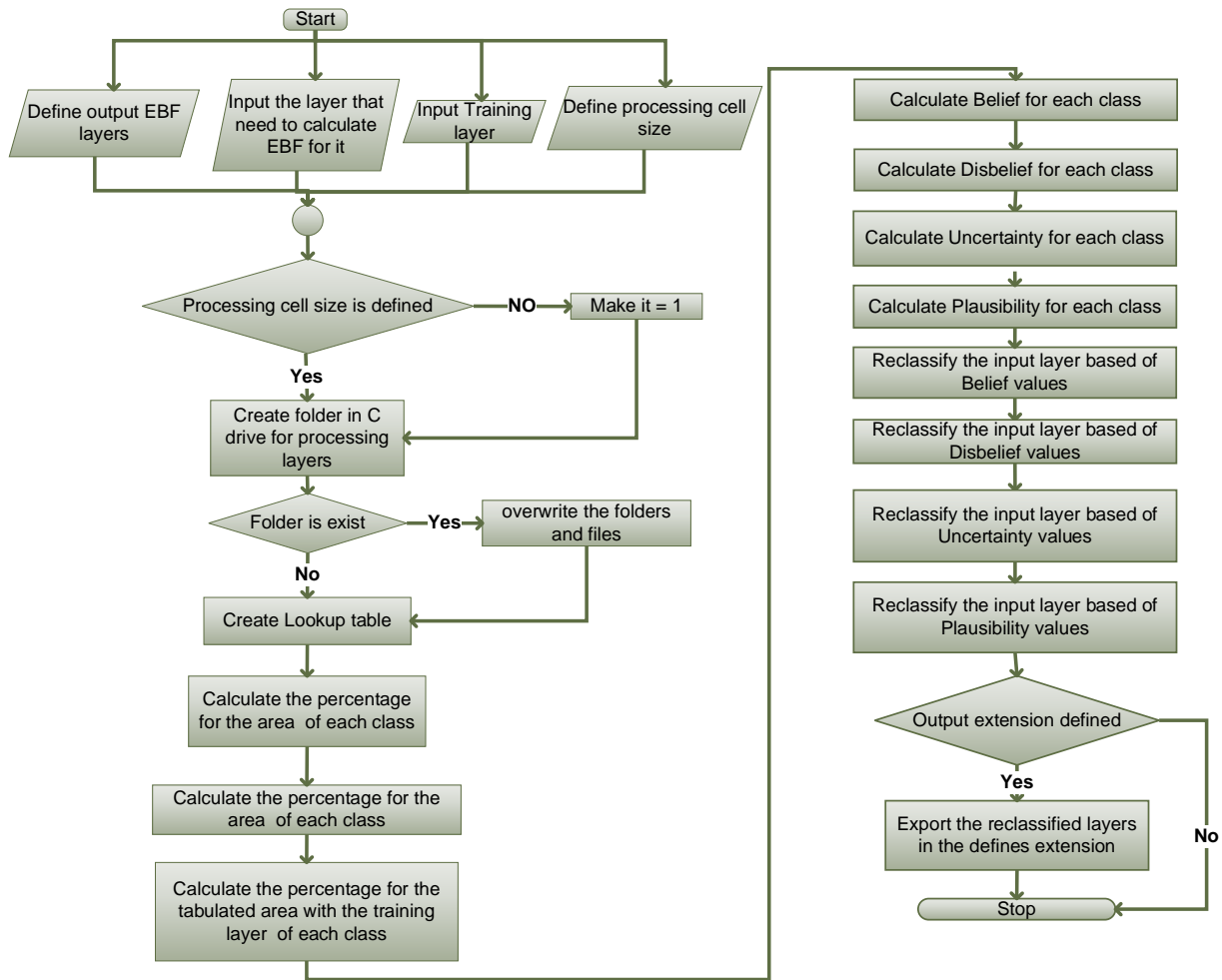


**Fig. 9.** Code flowchart of the EBF model.

520

521

522

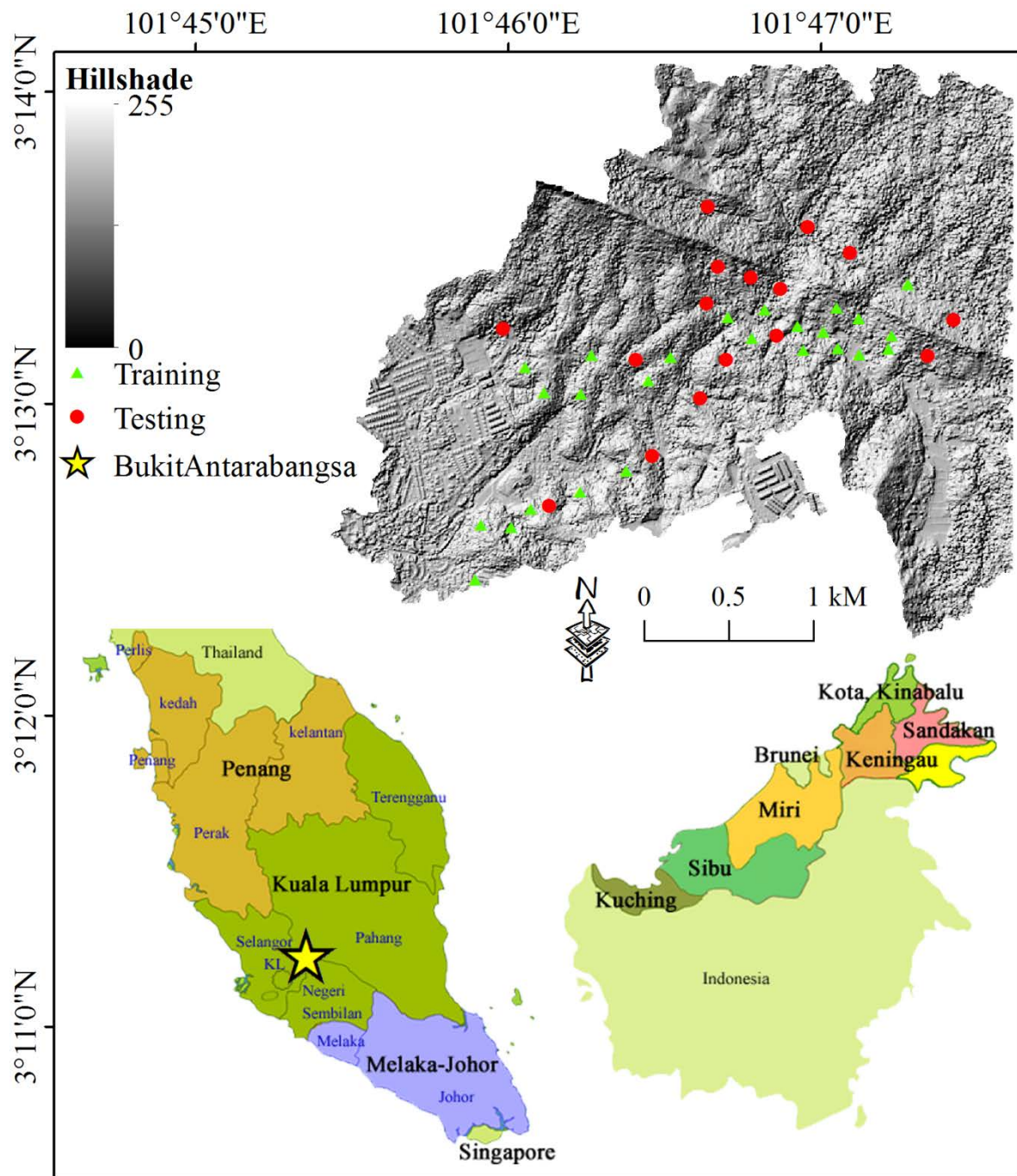
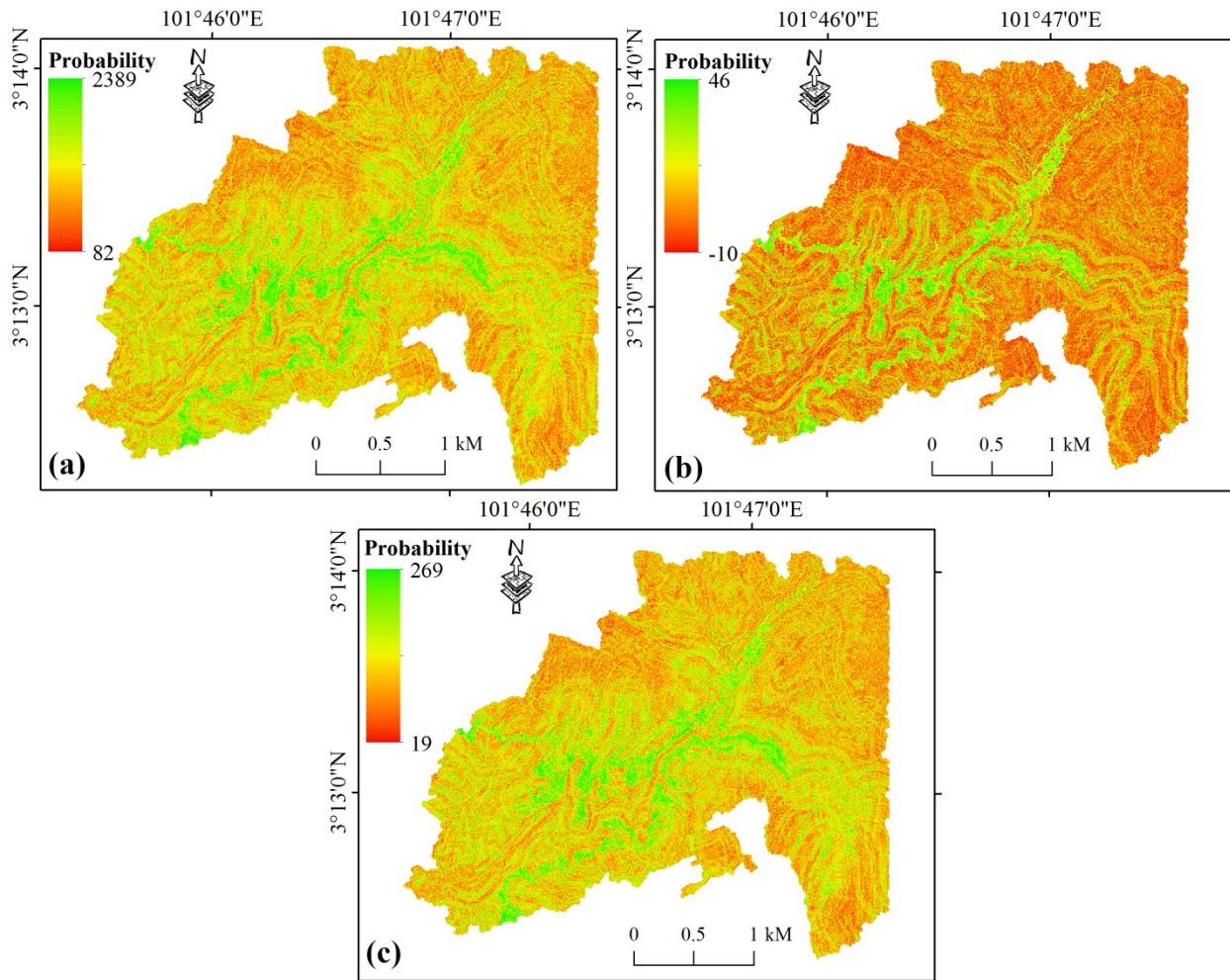


**Fig. 10.** Location of the pilot study area for testing the proposed ArcMAP tool.

523  
524  
525



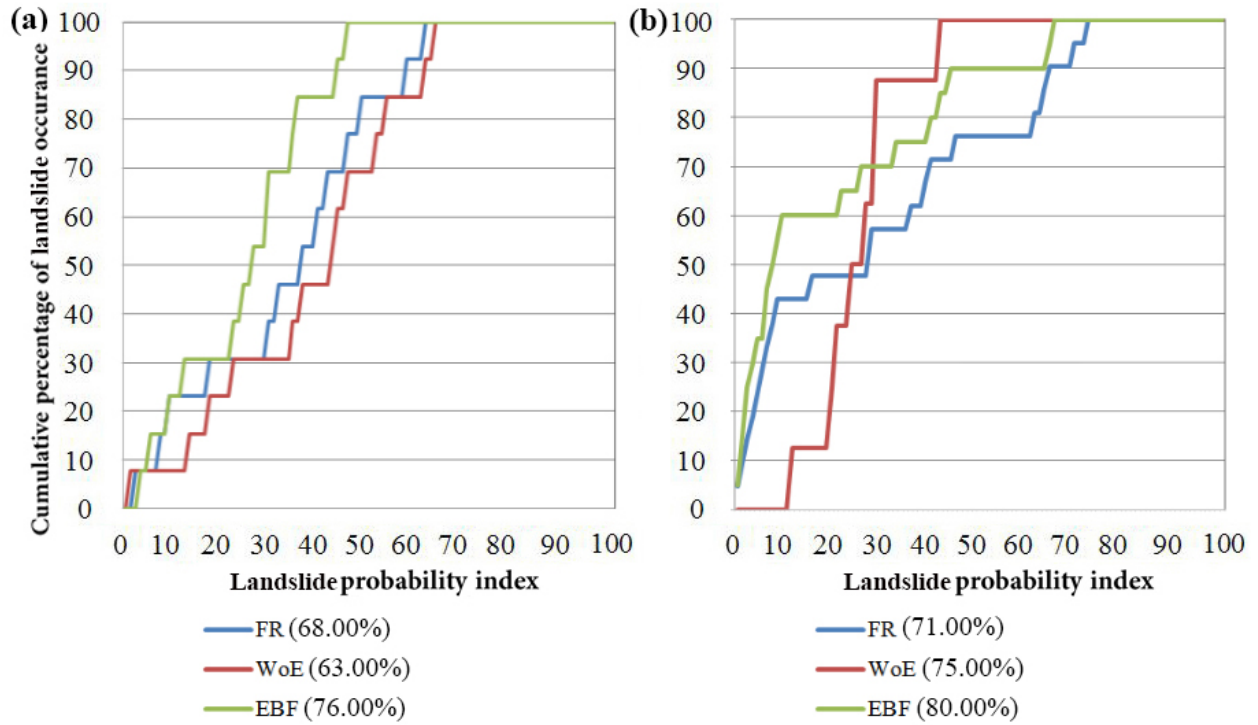
526

527

528

**Fig. 11.** Landslide susceptibility maps derived from a) FR, b) WoE, and c) EBF.





529

530 **Fig. 12.** Graphic representation of the cumulative frequency diagram presenting the cumulative  
 531 landslide occurrence (%; y-axis) in landslide probability index rank (%; x-axis): a) success rate,  
 532 and b) prediction rate.

533

534

535

536

537

538

539

540

541

542

543

544

545